Acta Oncologica, 2014; 53: 759–768

informa
healthcare

ORIGINAL ARTICLE

Response to neoadjuvant treatment of invasive ductal breast carcinomas including outcome evaluation: MRI analysis by an automatic CAD system in comparison to visual evaluation

JOACHIM BÖTTCHER[1,*], DIANE M. RENZ[2,*], DIRK-MICHAEL ZAHM[3], ALEXANDER PFEIL[4], EVA M. FALLENBERG[2], FLORIAN STREITPARTH[2], MARTIN H. MAURER[2], BERND HAMM[2] & FLORIAN J. ENGELKEN[2]

[1]*Institute of Diagnostic and Interventional Radiology, SRH Clinic Gera, Gera, Germany,* [2]*Department of Radiology, Charité University Medicine Berlin, Berlin, Germany,* [3]*Department of Gynecology, SRH Clinic Gera, Gera, Germany and* [4]*Department of Internal Medicine III, Friedrich-Schiller-University, Jena University Hospital, Jena, Germany*

Abstract

Background. The aim of this study was to evaluate imaging-based response to standardized neoadjuvant chemotherapy (NACT) regimen by dynamic contrast-enhanced magnetic resonance mammography (DCE-MRM), whereas MR images were analyzed by an automatic computer-assisted diagnosis (CAD) system in comparison to visual evaluation. MRI findings were correlated with histopathologic response to NACT and also with the occurrence of metastases in a follow-up analysis. *Patients and methods.* Fifty-four patients with invasive ductal breast carcinomas received two identical MRI examinations (before and after NACT; 1.5T, contrast medium gadoteric acid). Pre-therapeutic images were compared with post-therapeutic examinations by CAD and two blinded human observers, considering morphologic and dynamic MRI parameters as well as tumor size measurements. Imaging-assessed response to NACT was compared with histopathologically verified response. All clinical, histopathologic, and DCE-MRM parameters were correlated with the occurrence of distant metastases. *Results.* Initial and post-initial dynamic parameters significantly changed between pre- and post-therapeutic DCE-MRM. Visually evaluated DCE-MRM revealed sensitivity of 85.7%, specificity of 91.7%, and diagnostic accuracy of 87.0% in evaluating the response to NACT compared to histopathology. CAD analysis led to more false-negative findings (37.0%) compared to visual evaluation (11.1%), resulting in sensitivity of 52.4%, specificity of 100.0%, and diagnostic accuracy of 63.0%. The following dynamic MRI parameters showed significant associations to occurring metastases: Post-initial curve type before NACT (entire lesions, calculated by CAD) and post-initial curve type of the most enhancing tumor parts after NACT (calculated by CAD and manually). *Conclusions.* In the accurate evaluation of response to neoadjuvant treatment, CAD systems can provide useful additional information due to the high specificity; however, they cannot replace visual imaging evaluation. Besides traditional prognostic factors, contrast medium-induced dynamic MRI parameters reveal significant associations to patient outcome, i.e. occurrence of distant metastases.

Pre-operative, primary or also called neoadjuvant chemotherapy (NACT) is defined as the administration of anti-neoplastic agents to patients suffering from invasive breast carcinoma before receiving local treatment [1,2]. At the beginning, NACT was mainly used for the treatment of initially non-operable, locally advanced breast cancer [3]. The application of NACT has been extended and nowadays also includes early-stage carcinomas in order to downsize them and therefore to enable suitable breast conserving surgery in women, who would have initially received radical mastectomy [1,2]. NACT has been proven to improve overall as well as relapse-free survival, equivalent to adjuvant chemotherapy [1–3].

Besides cancer downsizing, another advantage of NACT is the unique opportunity to directly evaluate treatment-induced tumoral changes during and after therapy and therefore confirm its efficacy. Clinical

*The authors contributed equally to this work.

Correspondence: D. M. Renz, Department of Radiology, Charité University Medicine Berlin, Charitéplatz 1, 10117 Berlin, Germany. Tel: +49 30 450657147. Fax: +49 30 450557990. E-mail: diane.renz@charite.de

(Received 21 March 2013; accepted 20 September 2013)

ISSN 0284-186X print/ISSN 1651-226X online © 2014 Informa Healthcare
DOI: 10.3109/0284186X.2013.852688

examination, x-ray mammography, and ultrasonography are commonly used in clinical routine to assess the chemoresponsiveness, however, with only moderate correlations to the histologically verified response following breast surgery [4,5]. Dynamic contrast-enhanced magnetic resonance mammography (DCE-MRM) has been reported to monitor response to NACT better than conventional breast imaging modalities [4,5]. One major benefit of breast magnetic resonance imaging (MRI) is the simultaneous evaluation of morphologic and enhancement characteristics, which are associated with tumor angiogenesis and provide insights into tumor pathophysiology [6,7]. In order to reduce inter-observer variability and to receive kinetic data of whole contrast-enhancing lesions, dynamic enhancement is increasingly assessed by computer-assisted diagnosis (CAD) systems for DCE-MRM [8]. However, the efficacy of CAD systems in monitoring NACT, whereas dynamic MRI examinations were compared before versus after chemotherapy by a CAD technique, has been only investigated by DeMartini et al. [9] and Yi et al. [10], as far as we know.

The aim of this study was to evaluate the response to a standardized NACT regimen by breast MRI, considering dynamic and morphologic parameters as well as tumor size measurements. MR images before and after NACT were evaluated by a unique, fully-automatic CAD system as well as by two human blinded observers, whereas MRI findings were compared with histopathologically verified response to NACT. In an outcome analysis, all clinical, histopathologic, and DCE-MRM parameters were correlated with the occurrence of distant metastases.

Material and methods

Patients and treatment

This clinical trial was an extensive analysis of a longitudinal study design. The study design is in accordance with the guidelines of the local ethics committee and the Helsinki Declaration. Female patients were included, who experienced newly diagnosed, unilateral, initially non-metastatic invasive ductal breast carcinoma and received standardized NACT regimen. The patients showed findings on x-ray mammography and/or ultrasonography, which were suspicious for malignancy [Breast Imaging Reporting And Data System (BI-RADS), category 4 and 5]. Invasive breast cancer was diagnosed by core needle biopsy (14G) under ultrasonographic guidance, before the application of NACT was initiated. The patients received the first DCE-MRM before beginning of chemotherapy and the second DCE-MRM at completion of NACT directly before breast surgery. All patients experienced axillary lymph nodes, suspicious for malignant infiltration, on ultrasonography and on the first MRI examination on the same site as the unilateral invasive breast carcinoma. Patients with secondary breast carcinoma and with known history of malignant disease other than breast cancer were excluded. Further exclusion criteria were any contraindications against MRI or the application of MR contrast media.

Fifty-four patients fulfilled the strict inclusion criteria at a consecutive time period of 34 months. The mean age of the 54 women were 49.5 [standard deviation (SD) = 9.0] years ranging from 35 to 69 years at the time of the first MRI examination. More than half of the 54 patients (n = 30; 55.6%) presented multifocal malignant breast masses on the first DCE-MRM. The standardized regimen of NACT consisted of a combination of cyclophosphamide (500 mg/m^2), docetaxel (75 mg/m^2), and doxorubicin (50 mg/m^2) for six treatment cycles, administered every three weeks. The time interval between pre-therapeutic, first MRI examination and the first cycle of NACT ranged from 1 to 15 days (median 7, interquartile range, IQR, 5 days). After the completion of NACT, the second, pre-operative MRI examination was performed after a median duration of >3 weeks (25 days) after the last treatment cycle (range 20–33, IQR 5 days). The time interval between pre-operative MRI and breast surgery ranged from 1 to 14 days (median 6, IQR 3 days). The type of breast surgery was decided on the basis of the surgeon's recommendation and the patient's personal choice: In 40 of 54 (74.1%) patients, breast conservation surgery, and in 14 (25.9%) women, mastectomy was performed. All 54 patients had curative (R0) resection with histopathologic examination of margins showing no tumor cells. During breast surgery, all patients underwent axillary lymph node dissection. All 54 patients received radiation therapy after breast surgery and antihormonal treatment in case of positive hormonal receptor status.

MRI protocol

A standardized, identical protocol was used for both MRI examinations at 1.5T (Achieva®; Philips Healthcare, Best, The Netherlands) with bilateral breast coil and the patient in prone position. Three-dimensional (3D) gradient-echo T1-weighted axial sequences were acquired for dynamic imaging with the following parameters: repetition time (TR) 8.3 ms, echo time (TE) 4.6 ms, flip angle 12°, field of view (FOV) 320–360 mm, matrix 360×360, spatial resolution $0.7 \times 0.7 \times 2$ mm^3. Axial T2-weighted turbo-spin-echo sequences were performed before contrast medium application (TR 4618 ms, TE 120 ms,

flip angle 90°, FOV 320–360 mm, matrix 448×330, spatial resolution $0.7 \times 0.7 \times 3$ mm^3).

Gadoteric acid (Gd-DOTA, Dotarem®; Guerbet, Roissy CdG Cedex, France) was used as MR contrast medium at a dose of 0.1 mmol/kg body weight. Gd-DOTA was automatically administered at a flow rate of 3 mL/s by a power injector; the injection was followed by a 30-mL 0.9% saline flush with the same flow rate. Twenty seconds after the beginning of contrast medium injection, dynamic scanning was performed with the same sequence parameters and under identical tuning conditions; five post-contrast series were acquired with identical time intervals of 58 s. Native images were subtracted from post-contrast sequences to acquire subtraction images.

Imaging analysis

All MRI examinations were evaluated by an automatic CAD system (Breast MRI Carebox®; Bracco Imaging, Milan, Italy) and by two experienced radiologists, who analyzed the images in consensus (7 and 10 years experience in breast MRI interpretation). Dynamic and morphologic analysis was performed in accordance to the guidelines of the internationally accepted MRI BI-RADS atlas [11]. MR images were evaluated by CAD and visually in a blinded manner to clinical and radiological data as well as the acquisition time point, i.e. if the examinations were obtained before or after the application of NACT. The novel, fully-automatic CAD technique for breast MRI has been recently described and evaluated in detail, showing that it can reliably distinguish between malignant and benign masses with a diagnostic accuracy of 93.5% [12].

After motion correction and detection of contrast-enhancing lesions, the CAD system calculated several morphologic and dynamic features and linked these parameters to descriptions of the MRI BI-RADS atlas [11]. The CAD system performed dynamic signal intensity time curves for each detected, entire mass (average signal intensity values) and for its hot spot region, i.e. the location with maximum signal intensity. Manually, three regions of interests (ROIs; 3×3 voxels) were placed in the most enhancing part of the breast tumors and the mean signal intensity values were assessed. All signal intensity time curves were divided in an initial phase during the first two post-contrast sequences and a delayed, post-initial phase afterwards (continuous increase, plateau phenomenon, and washout type) [6,7,12]. For the final classification, all computer-extracted morphologic and dynamic parameters of each lesion were combined to calculate its probability of malignancy (morpho-dynamic index, MDI; range 0–100%) [12]. In the case of multifocality, the malignant lesion with the largest size was used as the target lesion for morphologic and dynamic MRI analysis as well as the evaluation by the Response Evaluation Criteria In Solid Tumors (RECIST) classification.

For the categorization based on the RECIST guidelines, the longest tumor diameter on pre-therapeutic DCE-MRM was visually compared with the corresponding post-therapeutic MRI examination [5]. The changes of tumor sizes resulted in four response categories according to the RECIST guidelines [5]: Complete response (CR), partial response (PR), stable disease (SD), and progressive disease (PD).

Histopathologic evaluation

Histopathologic diagnosis was performed by experienced breast pathologists. The carcinomas were categorized by the World Health Organization (WHO) classification. The clinical stage of the carcinomas was assessed according to the TNM classification. Tumor grades of the carcinomas were distinguished between well (grade 1), moderately (grade 2), and poorly (grade 3) differentiated. Estrogen and progesterone receptor (ER, PR) status was obtained at the initial cancer diagnosis following core biopsy; hormonal receptor status was defined as positive if $>10\%$ of the tumor cells exhibited immunohistochemical nuclear staining. Expression of human epidermal growth factor receptor 2 (HER2) was classified by dichotomizing: score 0 or $+1$ as receptor-negative, score $+2$ or $+3$ as receptor-positive. At the biopsy tissue sample, the proliferation rate of the carcinomas was furthermore assessed by Ki67 staining (Ki67 score, range 0–100%).

Following breast surgery, histopathologic response to NACT was assessed as follows [13]: 1) No residual malignancy, no vital cancer cells [complete pathologic response (CPR)]; 2) No invasive carcinoma, but persistent ductal carcinoma in situ (DCIS); and 3) Invasive cancer detected.

Follow-up analysis

Initial staging examinations included chest x-ray, ultrasonography of the abdomen, and bone scintigraphy, whereas none of the included patients experienced synchronous distant metastases. All 54 patients underwent clinical follow-up, which included x-ray mammography and breast ultrasonography every 6–12 months to exclude local tumor recurrence and a clinical examination including regular evaluation of serum tumor markers. In case of clinical disorders or symptoms, patients received chest x-ray, ultrasonography of the abdomen, bone scintigraphy, computed tomography, or MRI for imaging diagnosis. The

follow-up was performed for a duration of at least 24 months after the first breast MRI examination in 42 patients, who did not develop metachronous metastases within this observation period (median duration 34, range 24–53, IQR 18 months). In the remaining 12 patients, distant metastases were diagnosed after a median duration of 19 months (range 8–37, IQR 14 months). Within the observation period, none of the included patients experienced local tumor recurrence in the breast.

Statistical analysis

The statistical evaluation was performed by using SPSS version 19.0 for Windows (Chicago, IL, USA). For correlation analyses, Spearman's rank (for ordinal data) and Pearson's correlation coefficients (for interval parameters) were calculated. To examine if pre-therapeutic parameters changed significantly after the application of NACT, Wilcoxon signed rank tests were performed in the case of ordinal data. Paired and independent samples Student's t-tests were used to examine significant differences between means of two paired and independent samples with normal distribution, respectively. Pearson's χ^2-tests analyzed associations between categorical variables. Sensitivity, specificity, and diagnostic accuracy of MRI in comparison to histopathologic evaluation after neoadjuvant treatment were determined [14].

In the follow-up evaluation, associations between the occurrence of distant metastases and clinical, histopathologic and MRI parameters were evaluated by univariate analyses. In this context, Fisher's exact tests were calculated to examine associations between two variables in a 2×2 contingency table. Two samples Kolmogorov Smirnov tests were used for non-parametric analysis and Student's t-tests for interval parameters with normal distribution. Additionally, binomial logistic regression analysis was performed. P-values (two-sided) < 0.05 were considered in all calculations to indicate significant differences.

Results

Initial tumor characteristics

Based on the TNM classification, approximately three quarters (75.9%) of the 54 included invasive ductal breast carcinomas were categorized as clinical cancer stage IIB and IIIA before neoadjuvant treatment (Table I). The largest tumor diameters, measured on MRI before NACT, ranged from 17 to 92 mm (mean maximum diameter 35.3, SD 17.3 mm). Tumor grading and hormonal receptor status of the carcinomas are presented in Table I; their mean Ki67 value was 47.1% (SD 27.5%, range 10–90%).

Table I. Characteristics of invasive ductal breast carcinomas before neoadjuvant treatment (n = 54).

	Number	Percentage*
Initial, pre-therapeutic cancer stage		
IIA	5	9.3
IIB	24	44.4
IIIA	17	31.5
IIIB	5	9.3
IIIC	3	5.6
Initial tumor grading		
G1 (well differentiated)	0	0.0
G2 (moderately differentiated)	19	35.2
G3 (poorly differentiated)	35	64.8
Receptor status		
ER and PR positive	34	63.0
HER2 positive	19	35.2

ER, estrogen receptor; HER2, human epidermal growth factor receptor; PR, progesterone receptor.
*The percentages may not add up to 100.0% due to rounding.

Response to neoadjuvant chemotherapy

The results of the imaging-based response to NACT according to the RECIST guidelines in comparison to histopathologic response are summarized in Table II; the three cases with PD revealed new

Table II. Response to neoadjuvant chemotherapy of invasive ductal breast carcinomas assessed by RECIST (evaluation of post-therapeutic versus initial MRI) and by histopathologic analysis, including post-therapeutic tumor grading and cancer stage.

	Number	Percentage*
MRI response based on RECIST (n = 54)		
Complete response (CR)	17	31.5
Partial response (PR)	25	46.3
Stable disease (SD)	9	16.7
Progressive disease (PD)	3	5.6
Histopathologic response (n = 54)		
Complete pathologic response (CPR)	12	22.2
No invasive residues but persistent DCIS	6	11.1
Invasive ductal cancer detected	36	66.7
Post-therapeutic tumor grading (n = 42 DCIS and invasive ductal carcinomas)		
G1	3	7.1
G2	16	38.1
G3	23	54.8
Post-therapeutic cancer stage (n = 36 invasive ductal carcinomas)		
I	8	22.2
IIA	12	33.3
IIB	6	16.7
IIIA	4	11.1
IIIB	3	8.3
IIIC	3	8.3

DCIS, ductal carcinoma in situ; RECIST, response evaluation criteria in solid tumors.
*The percentages may not add up to 100.0% due to rounding.

malignancies in the breast. All carcinomas presented some therapy-induced regressive and/or reactive changes (e.g. fibrosis, necrosis, inflammatory changes) at histopathology after NACT. There was a significant correlation between response evaluation by RECIST and histopathology (Spearman's rank correlation coefficient $rs = 0.74$, $p < 0.001$). Visual MRI correctly detected complete pathologic response (CPR) in 11 of 12 cases (true-negatives). However, MRI resulted in six false-negative findings ($6/54 = 11.1\%$); the pathologic analysis of these six cases revealed the following findings: maximum 3 mm-sized invasive ductal carcinoma (G2), scattered nodules of a maximum 7 mm-sized invasive ductal carcinoma (G2), two low-grade (G1) DCIS lesions (14 and 11 mm maximum diameter), two intermediate-grade (G2) DCIS lesions (8 and 6 mm maximum diameter) with extensive fibrosis in the surrounding tissue. In one case with CPR, MRI demonstrated maximum 8 mm-sized mass in a patient with distinct background enhancement after completion of NACT, which was interpreted as residual cancer lesion (false-positive finding); this lesion was histopathologically confirmed as adenosis. Thus, visually evaluated DCE-MRM revealed sensitivity of 85.7%, specificity of 91.7%, and diagnostic accuracy of 87.0%.

The application of NACT resulted in downsizing of breast carcinomas with lower post-therapeutic cancer stages compared to the initial ones (Wilcoxon signed rank test, $p < 0.001$; Tables I and II). Post-therapeutic tumor grading of the invasive and intraductal carcinomas was also lower compared to the initial grading of the malignancies (Wilcoxon signed rank test, $p < 0.05$; Tables I and II). The largest tumor diameters of 36 on visual MRI correctly detected carcinomas were also decreased on post-therapeutic DCE-MRM (paired samples Student's t-test, $p < 0.001$; Figure 1): mean size 24.9, SD 17.7 mm. Regarding these 36 invasive and intraductal carcinomas, which were visible in both post-therapeutic, dynamic MRI sequences and histopathologic analysis, the mean tumor diameter, measured at histology, was

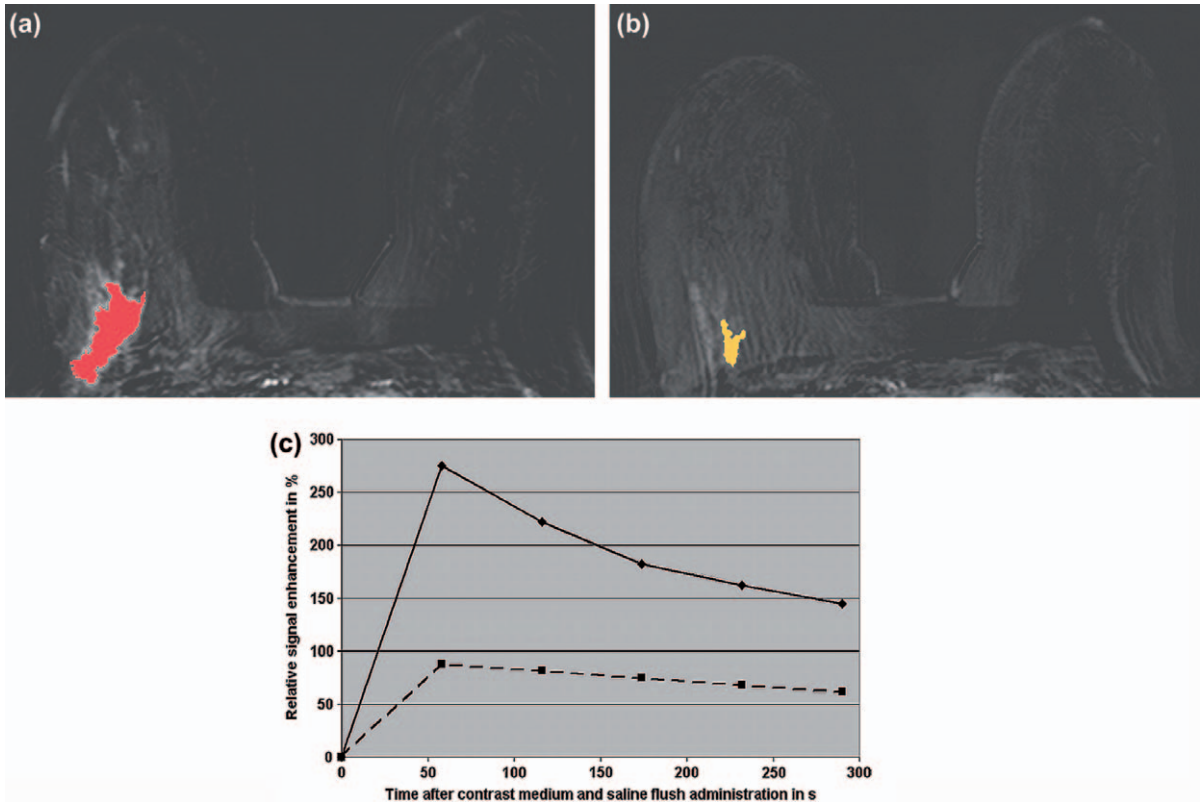

Figure 1. Invasive ductal carcinoma (G3) in the right breast of a 38-year-old patient before and after neoadjuvant chemotherapy (NACT). Before NACT, the CAD system coded the mass-like malignant lesion, but not the surrounding extensive intraductal component and the adjacent vessels (a), first subtraction image after contrast medium administration). The right breast reveals prominent vessels. After NACT, histopathology revealed persistent invasive ductal cancer (G3). The CAD system still coded the carcinoma, which size is decreased after neoadjuvant treatment (b), first subtraction image after contrast medium administration). The signal intensity time course of the hot spot region (c), i.e. the relative signal intensity in % over time in s, demonstrates before NACT a strong initial enhancement > 250% followed by a washout (continuous curve). After NACT, the signal intensity time course of the hot spot region (c) had an initial enhancement > 80% followed by a washout (discontinuous curve). Morphologically, the CAD system identified before and after NACT an irregular shape and a spiculated margin. The morpho-dynamix index, i.e. the probability of malignancy, decreased from initial 98% to 56% after NACT. Twenty-five months after initial breast cancer diagnosis, this patient suffered from bone, pleural, and liver metastases.

slightly, not significantly lower (mean maximum histologic diameter 23.2., SD 14.4 mm) compared to the mean assessments on MRI (independent samples Student's t-test, $p > 0.05$); the correlation between post-therapeutic, pre-operative MRI measurements and pathologic assessments of maximum tumor diameters was Pearson's correlation coefficient $r = 0.77$ ($p < 0.001$).

Changes of MRI parameters

Before neoadjuvant treatment, all 54 invasive breast carcinomas presented masses on MRI; all carcinomas were initially detected by the CAD system. The initial and post-initial curve types, as assessed by the CAD system (entire lesions and hot spot regions) and by manual ROI analysis, are presented in Table III. After neoadjuvant treatment, the CAD system detected 22 carcinomas. As 12 initially invasive ductal carcinomas revealed CPR after the application of NACT, the CAD system did not code 20 cases with residual invasive or intraductal cancer, identified at histopathology (false-negative findings; 20/54 = 37.0%). There was no false-positive finding of the CAD system after NACT, i.e. segmentation of an intramammary lesion with MDI > 50%. Thus, CAD evaluation of MR images reached sensitivity of 52.4%, specificity of 100.0%, and diagnostic accuracy of 63.0%.

Considering dynamic MRI parameters, the application of NACT resulted in lower initial signal increases compared to pre-therapeutic initial signal enhancement (Tables III and IV; Figure 1); this decrease was significant for the 22 carcinomas (entire lesions and hot spot regions), coded before and after NACT by CAD, and for the 36 visually detected carcinomas by ROI analysis (Wilcoxon signed rank tests, $p < 0.001$). Post-initial signal enhancement was also significantly different with more continuous and less washout curve types after NACT compared to pre-therapeutic DCE-MRM for all three evaluation methods (Wilcoxon signed rank tests, $p < 0.01$; Tables III and IV). Post-therapeutic initial and post-initial signal enhancement was significantly associated with assessment of response based on RECIST

Table III. Initial relative signal enhancement (percentage of signal intensity increase during the first 2 post-contrast dynamic sequences) and post-initial curve types (continuous increase, plateau phenomenon, washout sign) of invasive ductal breast carcinomas (n = 54) before neoadjuvant treatment, as calculated by the CAD system and manually by ROI analysis.

	Number	Percentage*
Entire lesions by CAD		
50–100%	8	14.8
100–150%	19	35.2
150–200%	20	37.0
200–250%	7	13.0
Continuous increase	9	16.7
Plateau phenomenon	28	51.9
Washout sign	17	31.5
Hot spot regions by CAD		
50–100%	3	5.6
100–150%	8	14.8
150–200%	9	16.7
200–250%	15	27.8
250–300%	11	20.4
>300%	8	14.8
Continuous increase	5	9.3
Plateau phenomenon	17	31.5
Washout sign	32	59.3
Manual ROI analysis		
50–100%	5	9.3
100–150%	7	13.0
150–200%	10	18.5
200–250%	17	31.5
250–300%	12	22.2
>300%	3	5.6
Continuous increase	6	11.1
Plateau phenomenon	19	35.2
Washout sign	29	53.7

CAD, computer-assisted diagnosis; ROI, region of interest.
*The percentages may not add up to 100.0% due to rounding.

Table IV. Initial relative signal enhancement (percentage of signal intensity increase during the first 2 post-contrast dynamic sequences) and post-initial curve types (continuous increase, plateau phenomenon, washout sign) of detected carcinomas after neoadjuvant treatment, as calculated by the CAD system and manually by ROI analysis.

	Number	Percentage*
Entire lesions by CAD (n = 22)		
<50%	4	18.2
50–100%	9	40.9
100–150%	9	40.9
Continuous increase	13	59.1
Plateau phenomenon	8	36.4
Washout sign	1	4.5
Hot spot regions by CAD (n = 22)		
50–100%	12	54.5
100–150%	5	22.7
150–200%	2	9.1
200–250%	1	4.5
250–300%	2	9.1
Continuous increase	9	40.9
Plateau phenomenon	6	27.3
Washout sign	7	31.8
Manual ROI analysis (n = 36)		
<50%	11	30.6
50–100%	15	41.7
100–150%	7	19.4
150–200%	2	5.6
200–250%	1	2.8
Continuous increase	21	58.3
Plateau phenomenon	8	22.2
Washout sign	7	19.4

CAD, computer-assisted diagnosis; ROI, region of interest.
*The percentages may not add up to 100.0% due to rounding.

guidelines (Spearman's rank correlation coefficients 0.52–0.67; $p < 0.05$).

Regarding morphologic descriptions by CAD on pre-therapeutic DCE-MRM, the majority of 54 target lesions (n = 28; 51.9%) presented an irregular shape; 12 masses (22.2%) were lobular, and 14 (25.9%) round/oval. The margins of the 54 target lesions were: 44.4% spiculated (n = 24), 35.2% irregular (n = 19), and 20.4% smooth (n = 11). After neoadjuvant treatment, the morphologic descriptions of the detected carcinomas did not significantly differ from their pre-therapeutic assessments, neither for the evaluation by CAD nor by the observers (Wilcoxon signed rank tests, $p > 0.05$). Assessments of dynamic and morphologic parameters were consistent between CAD and human evaluation for pre- and post-therapeutic MRI (Spearman's rank correlation coefficients 0.64–0.88; $p < 0.01$). The 54 target lesions showed a mean MDI of 87.8% (SD 10.3%, range 48–99%) before NACT. After neoadjuvant treatment, the MDI values of the by CAD detected 22 carcinomas were significantly lower: mean 62.0%, SD 15.9%, range 33–87% (paired samples Student's t-test, $p < 0.001$).

Follow-up analysis

The 12 patients, in whom distant metastases were diagnosed within the follow-up analysis, suffered from the following metastatic localizations: n = 3 pleural and pulmonary, n = 2 pleural, n = 2 pleural and bone, n = 2 bone, n = 1 cerebral, n = 1 bone, pleural and cerebral, and n = 1 bone, pleural, and liver. By performing univariate statistical analyses, some of all evaluated clinical, histopathologic, and MRI parameters demonstrated a significant association with the occurrence of metastases (listed in Table V; see also Figure 1); the binomial logistic regression analysis confirmed all of these parameters as significant independent predictors.

Table V. Results of univariate analyses considering clinical, histopathologic, and MRI parameters, which reveal significant associations with the occurrence of distant metastases in 54 patients with initial invasive ductal carcinomas.

	Occurrence of distant metastases within the follow-up period (n = 12 cases)	No occurrence of distant metastases within the follow-up period (n = 42 cases)	Statistical analyses and p-values (two-sided)
Clinical parameters			
Initial, pre-therapeutic cancer stage	IIB: 2; IIIA/B/C: 10	IIA/B: 27; IIIA/B/C: 15	Fisher's exact test; $p < 0.01$
Post-therapeutic cancer stage after NACT	IIA/B: 7; IIIA/B/C: 5	Missing (tumor T0/Tis): 18; I/IIA/IIB: 19; IIIA/B: 5	Fisher's exact test; $p < 0.01$
Histopathologic parameters			
Proliferation rate Ki67 value	Mean 60.8 ± 21.6%	Mean 43.2 ± 28.0%	Student's t-test; $p < 0.05$
Histopathologic response to NACT	No tumor or DCIS: 0; invasive carcinoma: 12	No tumor or DCIS: 18; invasive carcinoma: 24	Fisher's exact test; $p < 0.01$
Maximum histologic size (DCIS and invasive cancer) after NACT	Mean 29.4 ± 15.5 mm	Missing (no cancer): 12; Mean 17.7 ± 12.7 mm	Student's t-test; $p < 0.05$
MRI parameters			
Maximum size of target lesions before NACT	Mean 47.2 ± 19.8 mm	Mean 31.9 ± 15.1 mm	Student's t-test; $p < 0.05$
Maximum size of target lesions after NACT	Mean 33.6 ± 19.1 mm	Missing (not visible): 18 Mean 20.5 ± 15.5 mm	Student's t-test; $p < 0.05$
Cancer coded by CAD after NACT	Yes: 9; no: 3	Yes: 13; no: 29	Fisher's exact test; $p < 0.01$
Post-initial curve type before NACT: entire lesions calculated by CAD	Continuous: 2; plateau: 2; washout: 8	Continuous: 7; plateau: 26; washout: 9	Two samples KS test; $p < 0.05$
Post-initial curve type after NACT: hot spot regions calculated by CAD	Missing (not coded): 3; continuous: 2; plateau: 1; washout: 6	Missing (not coded): 29; continuous: 7; plateau: 5; washout: 1	Two samples KS test; $p < 0.05$
Post-initial curve type after NACT: by manual ROI analysis	Continuous: 3; plateau: 4; washout: 5	Missing (not visible): 18; continuous: 18; plateau: 4; washout: 2	Two samples KS test; $p < 0.05$

CAD, computer-assisted diagnosis; KS, Kolmogorov Smirnov; NACT, neoadjuvant chemotherapy; ROI, region of interest.
The data are presented as numbers of cases if no dimensions are indicated.

Discussion

The reliable imaging-based assessment of residual disease including accurate size measurement after neoadjuvant treatment is essential to initiate an optimum surgical approach and therefore to achieve high patient outcome. The main differences between our trial and previous investigations are the concomitant analysis of morphologic and dynamic MRI parameters before and after NACT by a unique, fully-automatic CAD system as well as by blinded human observers. Another benefit of our study is an additional analysis of patient outcome, whereas all included clinical, histopathologic, and MRI parameters have been analyzed as potential predictors. As one important result of our study, the specificity of DCE-MRM was higher than the sensitivity for visual as well as CAD evaluation. In non-treated breast carcinomas, DCE-MRM has been proven as the most sensitive imaging method approaching nearly 100% with in general lower specificity [6,12]. However, Yuan et al. [15] found in a meta-analysis of 25 trials (imaging evaluation either by human readers or by CAD) that breast MRI reached overall specificity of 91% and relatively lower sensitivity of 63% in predicting PCR after NACT. In a review including > 1900 patients with imaging analysis solely by human readers, Wu et al. [16] came to the conclusion that diffusion weighted imaging (DWI) was highly sensitive (overall sensitivity 93%) and dynamic breast MRI high specific (overall specificity 91%) in predicting pathologic response to NACT.

The higher rate of false-negative compared to false-positive findings following NACT can occur due to therapy-induced regression and extensive tumor shrinkage resulting in scattered, small cancer foci, which can be too small or too weakly enhancing to be reliably visible on DCE-MRM [15,17,18]. Extensive regression can also cause an overestimation of breast tumor sizes on MRI compared to histopathology, as fibrotic or inflammatory changes can lead to weak signal enhancement [14,17,18]. Thus, slightly higher means of largest tumor diameters have been assessed by MRI in comparison to histopathology in our investigation, in concordance with the findings of Belli et al. [14] and Wasser et al. [18]. Despite the slight overestimation, the correlation of tumor size assessments by visual MRI in comparison to histopathology is relatively high, in our study calculated with 0.77, in accordance with published correlation coefficients ranging from 0.60 to 0.97 [5,9,14,18].

Another reason for the high rate of false-negatives and thus the relatively low sensitivity of DCE-MRM after NACT, found by visual as well as CAD evaluation, is presumably the antiangiogenic effect of neoadjuvant medication, such as docetaxel [15,19]. This antiangiogenic effect is caused by tumor and endothelial cell death, resulting in vessel damages and reduced production of angiogenic factors, e.g. vascular endothelial growth factor (VEGF), and hence less tumoral vascularization and signal enhancement [15,19]. Our visually assessed sensitivity of DCE-MRM is comparable with the sensitivity of 90.5% found by Belli et al. [14]; however, the visually assessed specificity was very high with 100.0% in this trial [14]. In a subgroup evaluation of the meta-analysis by Yuan et al. [15], the specificity values of breast MRI were lower in studies with PCR rates > 20% (in our study 22.2%) than in those with PCR rates < 20% (8.9% reported by Belli et al. [14]).

One major advantage of MRI is the possibility to evaluate contrast medium-induced dynamic, morphologic, and size assessments as response criteria to neoadjuvant treatment [6,15,20]. As far as we know, differences of morphologic MRI parameters between DCE-MRM before versus after NACT have not been evaluated so far. According to our findings, morphologic tumor descriptions do not change from pre- to post-therapeutic DCE-MRM, in contrast to dynamic MRI parameters. The change of dynamic initial and post-initial signal enhancement and the associations of dynamic parameters to response to NACT assessed by RECIST have been detected for visual and CAD evaluation in the same patient cohort; these dynamic changes and associations are in concordance with published results with sole visual evaluation of MR images [20,21].

Thus, therapy-induced changes of dynamic MRI parameters and their associations with response to NACT by RECIST seem to occur independently from the used measurements methods. In the investigation by DeMartini et al. [9], whereas enhancement curves were compared before versus after NACT solely by a semi-automatic CAD system, a significant decrease of washout enhancement has been found in residual carcinomas with < 5 mm histopathologic size. However, the false-negative rate of the CAD system, which used an enhancement threshold of 100%, was 53.8% [9]. The automatic CAD system with an adaptive instead of a fixed threshold resulted in a false-negative rate of 37.0% (20 of 54 cases) in our study. Thus, the major disadvantage of CAD systems after the application of NACT seems to be the higher false-negative rates compared to human readers, due to decreased tumoral enhancements. The carcinomas, which could be visually detected in the dynamic sequences, but were not coded by the CAD system after NACT, mostly revealed initial signal enhancement < 50% followed by continuous increase by manual ROI analysis. Nevertheless, CAD systems can complement the assessment of breast carcinomas before and after

NACT application, due to specificity of 100% in our trial. Further benefits are the possibility to calculate tumor volumes and to obtain dynamic data not solely from a part, but from the entire enhanced lesions [8–10,12,22].

In the follow-up analysis, post-initial enhancement of the entire lesions (assessed by CAD before NACT) significantly differed between patients with versus without metastases. Disease-related death of breast cancer is in general more associated with distant than local tumor recurrence [2,23]. Some investigations evaluated the prognostic value of pre-therapeutic dynamic MRI parameters. In a detailed, prospective, observational study, Baltzer et al. [24] identified washout enhancement type, which was assessed by semi-automatic CAD analysis considering the most suspect curve, as independent predictor for the occurrence of distant metastases. However, post-initial curve types of the most enhancing parts of our evaluated advanced breast carcinomas (in contrast to the post-initial curves of the entire lesions) were not significantly different before NACT, as washout curves of the most enhancing tumor parts were predominant in both patient cohorts (with vs. without metastases) on pre-therapeutic DCE-MRM. Pickles et al. [25] found significant associations of initial and post-initial pre-therapeutic dynamic MRI characteristics with overall and disease-free survival in breast cancer patients undergoing NACT. We integrated a relation analysis of post-therapeutic MRI parameters, whereas post-initial curve types of the most enhancing tumor parts (assessed by CAD and manual ROI analysis) and detection of lesions by CAD after NACT, by using gadoteric acid with very safe pharmacologic profile, were significantly associated with the occurrence of distant metastases. In the study by Yi et al. [10], who evaluated the dynamic MRI parameters before and after NACT by a commercialized CAD system, a smaller reduction in washout component of the whole tumors after ending of neoadjuvant treatment was a significant independent predictor for worse recurrence-free and overall survival.

Thus, besides traditional prognostic factors (cancer stage, tumor size before and after NACT, histopathologic response to NACT), contrast medium-induced dynamic MRI parameters can reveal significant associations to patient outcome after the application of neoadjuvant treatment; RECIST-based assessment on chemotherapeutic response, however, was not significantly related to occurrence of metastases in our investigation. In contrast to published results [23,25], high tumor grade and negative ER/PR status did not reach statistical significance in our study, but showed tendency (data not shown). The Ki67 proliferation status presented significant association with metachronous metastases; Caudle et al. [23] also reported that high Ki67 score was related to breast cancer progression during NACT.

There are some limitations of our study. As the inclusion criteria implicated strict and homogeneous study criteria, only a limited number of patients could be included. As the common clinical practice implements imaging solely in case of clinical symptoms or irregularities and no regular screening examinations looking for distant metastases, some patients might had occult metastases, which had not been diagnosed within the follow-up period. Tumor size changes have been assessed by the in clinical practice commonly used RECIST guidelines based on T1-weighted dynamic imaging [5,20,21]. T2-weighted MR imaging has not been specifically considered; however, post-therapeutic visual appearance of the carcinomas in T2-weighted imaged revealed significant associations with response to NACT (imaging-based by RECIST and by histopathologic verification; data not shown). Takeda et al. [22] reported that CAD-calculated changes of tumor volumes resulted in significantly higher inter-observer concordance compared to conventional measurements of the longest tumor diameters. As more false-negative findings occurred by CAD analysis compared to visual evaluation, the tumor sizes were considered by manual assessment of the longest diameters in our study. In future, CAD systems, including standardized tumor volume measurements, should be technically improved to reduce the rate of false-negative findings and to achieve an increased sensitivity for evaluation of response to NACT.

Conclusions

Dynamic contrast-enhanced breast MRI enables accurate evaluation of response to neoadjuvant treatment in comparison to histopathologic verification. CAD systems can complement the visual evaluation of MR images before and after neoadjuvant treatment and can provide useful additional information due to the high specificity and the possibility to obtain dynamic data not solely from a part, but from the entire enhanced lesions. However, CAD systems cannot replace MR imaging evaluation by human readers due to their high rate of false-negative findings. Besides traditional prognostic factors, contrast medium-induced dynamic MRI parameters reveal significant associations to patient outcome, i.e. occurrence of distant metachronous metastases.

Acknowledgments

The authors thank Toni Vomweg, MD, Heiner Faber, and Dirk Iwamaru, PhD (all Bingen, Germany) for technical support.

Declaration of interest: The authors report no conflicts of interest. The authors alone are responsible for the content and writing of the paper.

The study has been applied for a financial grant, whereas the final decision is pending at the time of publication. The data and the results of the study were independently obtained, and the investigators had exclusive control of the design, the data and the results of the study. Thus, there was no conflict of interest regarding the study.

References

[1] Rastogi P, Anderson SJ, Bear HD, Geyer CE, Kahlenberg MS, Robidoux A, et al. Preoperative chemotherapy: Updates of National Surgical Adjuvant Breast and Bowel Project Protocols B-18 and B-27. J Clin Oncol 2008;26:778–85.

[2] Mauri D, Pavlidis N, Ioannidis JP. Neoadjuvant versus adjuvant systemic treatment in breast cancer: A meta-analysis. J Natl Cancer Inst 2005;97:188–94.

[3] Swain SM, Sorace RA, Bagley CS, Danforth DN Jr, Bader J, Wesley MN, et al. Neoadjuvant chemotherapy in the combined modality approach of locally advanced nonmetastatic breast cancer. Cancer Res 1987;47:3889–94.

[4] Croshaw R, Shapiro-Wright H, Svensson E, Erb K, Julian T. Accuracy of clinical examination, digital mammogram, ultrasound, and MRI in determining postneoadjuvant pathologic tumor response in operable breast cancer patients. Ann Surg Oncol 2011;18:3160–3.

[5] Londero V, Bazzocchi M, Del Frate C, Puglisi F, Di Loreto C, Francescutti G, et al. Locally advanced breast cancer: Comparison of mammography, sonography and MR imaging in evaluation of residual disease in women receiving neoadjuvant chemotherapy. Eur Radiol 2004;14:1371–9.

[6] Kuhl CK. Current status of breast MR imaging. Part 2. Clinical applications. Radiology 2007;244:672–91.

[7] Renz DM, Diekmann F, Schmitzberger FF, Pietsch H, Fallenberg EM, Durmus T, et al. Pharmacokinetic approach for dynamic breast MRI to indicate signal intensity time curves of benign and malignant lesions by using the tumor flow residence time. Invest Radiol 2013;48:69–78.

[8] Dorrius MD, Jansen-van der Weide MC, van Ooijen PM, Pijnappel RM, Oudkerk M. Computer-aided detection in breast MRI: A systematic review and meta-analysis. Eur Radiol 2011;21:1600–8.

[9] DeMartini WB, Lehman CD, Peacock S, Russell MT. Computer-aided detection applied to breast MRI: assessment of CAD-generated enhancement and tumor sizes in breast cancers before and after neoadjuvant chemotherapy. Acad Radiol 2005;12:806–14.

[10] Yi A, Cho N, Im SA, Chang JM, Kim SJ, Moon HG, et al. Survival outcomes of breast cancer patients who receive neoadjuvant chemotherapy: Association with dynamic contrast-enhanced MR imaging with computer-aided evaluation. Radiology 2013;268:662–72.

[11] American College of Radiology. Breast imaging reporting and data system (BI-RADS) MRI atlas. 1st ed. Reston, VA: American College of Radiology; 2003.

[12] Renz DM, Böttcher J, Diekmann F, Poellinger A, Maurer MH, Pfeil A, et al. Detection and classification of contrast-enhancing masses by a fully automatic computer-assisted diagnosis system for breast MRI. J Magn Reson Imaging 2012;35:1077–88.

[13] Chen JH, Feig B, Agrawal G, Yu H, Carpenter PM, Mehta RS, et al. MRI evaluation of pathologically complete response and residual tumors in breast cancer after neoadjuvant chemotherapy. Cancer 2008;112:17–26.

[14] Belli P, Costantini M, Malaspina C, Magistrelli A, Latorre G, Bonomo L. MRI accuracy in residual disease evaluation in breast cancer patients treated with neoadjuvant chemotherapy. Clin Radiol 2006;61:946–53.

[15] Yuan Y, Chen XS, Liu SY, Shen KW. Accuracy of MRI in prediction of pathologic complete remission in breast cancer after preoperative therapy: A meta-analysis. Am J Roentgenol 2010;195:260–8.

[16] Wu LM, Hu JN, Gu HY, Hua J, Chen J, Xu JR. Can diffusion-weighted MR imaging and contrast-enhanced MR imaging precisely evaluate and predict pathological response to neoadjuvant chemotherapy in patients with breast cancer? Breast Cancer Res Treat 2012;135:17–28.

[17] Kim HJ, Im YH, Han BK, Choi N, Lee J, Kim JH, et al. Accuracy of MRI for estimating residual tumor size after neoadjuvant chemotherapy in locally advanced breast cancer: Relation to response patterns on MRI. Acta Oncol 2007; 46:996–1003.

[18] Wasser K, Sinn HP, Fink C, Klein SK, Junkermann H, Lüdemann HP, et al. Accuracy of tumor size measurement in breast cancer using MRI is influenced by histological regression induced by neoadjuvant chemotherapy. Eur Radiol 2003;13:1213–23.

[19] Grant DS, Williams TL, Zahaczewsky M, Dicker AP. Comparison of antiangiogenic activities using paclitaxel (taxol) and docetaxel (taxotere). Int J Cancer 2003; 104:121–9.

[20] Siegmann KC, Müller KT, Vogel U, Krauss K, Claussen CD. MR imaging of the breast before and after neoadjuvant treatment – enhancement characteristics and T2 signal intensity of breast cancers and breast parenchyma. Rofo 2010; 182:493–500.

[21] Nagashima T, Sakakibara M, Nakamura R, Arai M, Kadowaki M, Kazama T, et al. Dynamic enhanced MRI predicts chemosensitivity in breast cancer patients. Eur J Radiol 2006;60:270–4.

[22] Takeda K, Kanao S, Okada T, Kataoka M, Ueno T, Toi M, et al. Assessment of CAD-generated tumor volumes measured using MRI in breast cancers before and after neoadjuvant chemotherapy. Eur J Radiol 2012;81: 2627–31.

[23] Caudle AS, Gonzalez-Angulo AM, Hunt KK, Liu P, Pusztai L, Symmans WF, et al. Predictors of tumor progression during neoadjuvant chemotherapy in breast cancer. J Clin Oncol 2010;28:1821–8.

[24] Baltzer PA, Zoubi R, Burmeister HP, Gajda M, Camara O, Kaiser WA, et al. Computer assisted analysis of MR-mammography reveals association between contrast enhancement and occurrence of distant metastasis. Technol Cancer Res Treat 2012;11:553–60.

[25] Pickles MD, Manton DJ, Lowry M, Turnbull LW. Prognostic value of pre-treatment DCE-MRI parameters in predicting disease free and overall survival for breast cancer patients undergoing neoadjuvant chemotherapy. Eur J Radiol 2009; 71:498–505.